

Published in final edited form as:

*Angew Chem Int Ed Engl.* 2011 September 26; 50(40): 9365–9369. doi:10.1002/anie.201103641.

## Supramolecular Nanofibers and Hydrogels of Nucleopeptides

Xinming Li, Yi Kuang, Hsin-Chieh Lin, Yuan Gao, Junfeng Shi, and Bing Xu\*

Bing Xu: bxu@brandeis.edu

\*Department of Chemistry, Brandeis University, 415 South St., Waltham, MA 02454, USA, Fax: (+) 01-781-736-5201

### Keywords

supramolecular; nanofibers; hydrogels; biocompatible; nucleopeptides

This communication reports the integration of nucleobases with small peptides generates a novel kind of nucleopeptides as biocompatible and biostable supramolecular hydrogelators. As a class of molecules that contain both nucleobases and amino acids, nucleopeptides bear considerable biological and biomedical importance.[1] Naturally occurring nucleopeptides, such as willardiine-containing nucleopeptides and peptidyl nucleosides, are antibiotics against microorganisms.[2] A number of unnatural nucleobase containing peptides, such as peptide nucleic acids (PNA), have found successful applications in biology and biomedicine (as an analog of DNA).[3], [4] Such biological significances render nucleopeptides as attractive targets for heterocyclic chemistry and useful molecules for studying biology, which has achieved considerable success.[5] There is, however, little work to use nucleopeptides for developing novel class of materials.[6] Thus, we decide to explore the potential of nucleopeptides to serve as building blocks for biomaterials. Among many possible choices of the types of materials, we chose to generate hydrogels[7] of nucleopeptides for two simple reasons: (i) supramolecular hydrogels, resulted from molecular self-assembly in water that form entangled nanofibers, have exhibited considerable promises for applications in biomedicine because of the inherent biocompatibility and biodegradability associated with the supramolecular nanofibers;[8] (ii) despite their versatility and importance, small nucleopeptides have been hardly explored for hydrogels. Thus, the primary goal of this work is to design, synthesize, and evaluate molecular hydrogelators[7a, 7b, 9] made of nucleopeptides.

Despite the existence of several well-characterized forms of nucleopeptides (chiral nucleopeptides, achiral nucleopseudopeptides, or peptidyl and amino nucleosides),[1b] it is unknown which types of nucleopeptides would be optimal for generating molecular hydrogelators that form nanofibers and hydrogels. Based on that the dipeptide, L-Phe-L-Phe (FF), is able to form nanotube structures[10] and that aromatic rings interact with neighboring nucleobases to stabilize designed DNA structures,[4a] we hypothesize that the conjugation of FF with a nucleobase should lead to a molecular hydrogelator. Such a rationale turns out to be valid. As shown in Scheme 1, the connection of a nucleobase (adenine, guanine, thymine, or cytosine) to the dipeptides segment (FF), affords a novel series of nucleopeptides (**1**) as hydrogelators that self-assemble in water to form nanofibers and produce hydrogels at the concentration of 2.0 wt% and pH around 5. Molecular mechanics (MM) calculation indicates that the Hoogsteen interactions among nucleobases promote the formation of the nanofibers. The conjugation of a tyrosine phosphate to **1** yields

another group of nucleopeptides, precursors **2**, which undergo catalytic dephosphorylation to generate hydrogelators **3** that result in supramolecular nanofibers and hydrogels at low concentration (2.0 wt%) and physiological pH. Surprisingly, both **2** and **3** exhibit significant resistance to proteinase K, a powerful digestive enzyme. This result unambiguously confirms the unique advantage of nucleobase. Moreover, circular dichroism (CD) experiment and rheological measurement indicate that the nucleobases of the nucleopeptidic hydrogelators, after self-assembly, are able to interact with the nucleic acids through Watson-Crick H-bonding. Because nucleobases are an important class of biofunctional motifs, this work not only illustrates the first example of nucleopeptides as hydrogelators made by an enzymatic reaction, but also provides a facile way to explore the potential applications of nucleopeptides as biomaterials, which may lead to a new and general platform to examine specific biological functions (e.g., binding to DNA and RNA) of a dynamic supramolecular system that is able to interact with both proteins and nucleic acids.

Fig. 1a shows the typical synthetic route exemplified by the process for making the hydrogelators based on adenine. Following the procedures reported by Nieddu[11] for making nucleobase acetic acids, we first synthesized bis(tert-butyloxycarbonyl) (bis-Boc) protected adenine, (*N*<sup>6</sup>-bis-Boc-adenine-9-yl)-acetic acid (**4**). After being activated by *N*-hydroxysuccinimide (NHS), **4** reacts with L-Phe to afford **5**, which undergoes the same NHS activation and phenylalanine coupling to give the key intermediate **6**. Subsequent removal of the Boc-protecting groups with trifluoroacetic acid (TFA) yields the nucleopeptides (**1A**) in 47% total yield. Encouraged by that **1A**, acting as a hydrogelator, self-assembles to form nanofibers with the diameter of 16 nm (Fig. 2a) and results in a hydrogel at the concentration of 2.0 wt% and pH of 5.0, we used the NHS-activated intermediate **6** to react with L-Tyr-phosphate to obtain **7**, which forms precursor **2A** after the deprotection of the Boc groups. The dephosphorylation process of precursor **2A** catalyzed by an enzyme (Fig. 1b) leads to a translucent hydrogel of nucleopeptide **3A** (Table 1) at the physiological pH. <sup>31</sup>P NMR study confirms that the precursor (**2A**) completely transforms into the hydrogelator (**3A**) in 12 hr after the addition of alkaline phosphatase (ALP) (Fig. S2), and the TEM images (Fig. 2) of the negative stained hydrogel of **3A** reveals nanofibers with a width of 20 nm, confirming that nanofibers of **3A** act as the matrices to sustain the hydrogel (with a storage modulus around 2082 Pa at 2.0 wt%).

The formation of the nanofibers and the hydrogel of **1A** or **3A** indicates that the direct attachment of a purine or pyrimidine base to a small peptide is a valid approach to design hydrogelator of nucleopeptides. To examine the generality of this approach, we used the synthetic procedures similar to Fig. 1a to produce the nucleopeptides consisting of other nucleobases (**G**, **T**, or **C**) and examined their capability to form nanofibers and hydrogels. As revealed by TEM (Fig. 2), hydrogelators **1G**, **1T** and **1C** self-assemble to form nanofibers with the width of 15, 9, and 10 nm, respectively, and the nanofibers entangle to trap water and result in the hydrogels (Table 1) at the concentration of 2.0 wt% and slight acid condition (pH 5.0).

Like **2A**, precursors **2G** and **2T**, at 2.0 wt% and pH 7.4, upon the addition of ALP (10 U), turn into hydrogelators **3G** and **3T**, respectively. This enzymatic conversion leads to the formation of nanofibers **3G** and **3T** and results in the corresponding hydrogels shown in Table 1. TEM reveals that the diameters of the nanofibers of **3G** (14 nm) and **3T** (9 nm) are similar to those of the nanofibers of **1G** and **1T**, respectively. At the concentration of 2.0 wt % and pH 7.4, **3C** self-assembles to afford both nanoparticles (11 nm) and short, thin nanofibers (4 nm in diameter and about 200 nm long), but fails to form well-defined nanofiber networks to provide effective matrices that warrant a hydrogel of **3C**.

We measured the rheological properties of the hydrogels to gain further insight on their characteristics. As shown in Table 1, among them, the hydrogel of **1G** exhibits the highest storage modulus (12.6 KPa), the hydrogels of **1A** and **1T** possess relatively high storage moduli of 8.1 KPa and 6.3 KPa, respectively, and the hydrogel of **1C** has the lowest storage modulus (26 Pa). The storage moduli of the hydrogels of **3G** and **3T** are 682 Pa and 2.9 Pa, respectively, indicating that the hydrogel of **3T** possesses much weaker mechanical strength than those of the hydrogels **3A** and **3G** (Table 1). The relatively high storage moduli of hydrogels of **1A**, **1G**, **3A**, and **3G** may stem from that purine bases favor the formation of Hoogsteen base pair,[12] in addition to strong  $\pi$ - $\pi$  interaction of purine nucleobases that contain two fused five- and six-member heterocyclic rings. Moreover, the lower storage moduli of the hydrogels of **3** than those of the corresponding hydrogels of **1** suggest that the presence of tyrosine may reduce the efficiency of the non-covalent interactions required for the stabilization of self-assembled nanostructures, thus resulting in a relatively weak viscoelastic property of those hydrogels.

Furthermore, the addition of an oligomeric deoxyadenosine ( $A_{10}$ ) to the hydrogel of **1T** or **3T** results in a more stable hydrogel (Figs. S3, S6), as demonstrated by the increase of storage modulus ( $G'$ ) from 6.3 KPa (of hydrogel **1T**) to 14.3 KPa (of the hydrogel of **1T** and  $A_{10}$ ), or from 2.9 Pa (of hydrogel **3T**) to 12.0 Pa (of the hydrogel of **3T** and  $A_{10}$ ) (Fig. S6). This result suggests that Watson-Crick interactions between the self-assembly of **1T** (or **3T**) and  $A_{10}$  favor molecular aggregation and enhance the mechanical strength of the hydrogels. To further examine Watson-Crick H-bonding between complementary nucleobases among the hydrogelators, we use hydrogelators of **1T** and **1A** (or **3T** and **3A**) to prepare a mixed hydrogel and find that the increase of the storage modulus ( $G'$ ) from 6.3 KPa (of hydrogel **1T**) to 18 KPa (of the hydrogel of **1T** and **1A**), or from 2.9 Pa (of hydrogel **3T**) to 150 Pa (of the hydrogel of **3T** and **3A**). The mixed hydrogel of the mismatched nucleobases (i.e., (**1T** and **1G**) or (**1T** and **1C**)) exhibits, however, little increase of the storage moduli (Fig. S8) in comparison to that of hydrogel **1T**. These results indicate that these nucleopeptidic hydrogelators preserve Watson-Crick interaction of the nucleobases.

We used circular dichroism (CD) to study the superstructures of these nanofibers of self-assembled nucleopeptides in the gel phase. The hydrogels of **1** all give a common feature of  $\beta$ -sheet structure according to the CD spectra with a positive peak near 195 nm and a negative peak around 210 nm (Fig. S3), suggesting these nucleopeptides arrange into  $\beta$ -sheet-like configurations. The hydrogels of **3A**, **3G**, and **3T** display the common feature of the CD spectra with a positive peak near 195 nm and a negative peak around 210 nm, also suggesting that the nucleopeptides adopt  $\beta$ -sheet-like configurations. The CD spectrum of **3C** solution exhibits a positive peak near 203 nm and a negative peak around 215 nm, which red-shifts regarding to those in typical  $\beta$ -sheet. The red-shifted  $\beta$ -sheet signal likely associates with a twisted structure as opposed to the standard planar  $\beta$ -sheet, agreeing with the fact that the increase in  $\beta$ -sheet twisting causes disorder and results in the short nanofibers and the nanoparticles, which leads to weak mechanical strength.[13] Overall, the signals of  $\beta$ -sheet (i.e., transitions at 195 nm~225 nm) of **1** are stronger than those of **3**, following the trends that the storage moduli of **1** are larger than those of **3**. The CD signals with broad bands around 300 nm among the hydrogels **1** and **3** likely originate from the formation of mesophases of hydrogelators because they locate far from the chromophoric absorption region (ca. 270 nm) of the hydrogelators (Fig. S4).

Similar to other nucleobase-containing small molecules that bind with nucleic acids through Watson-Crick interaction,[14] hydrogelator **1T** or **3T** also binds to oligomeric deoxyadenosine (e.g.,  $A_{10}$ ), which results in the distinctive changes in the CD spectra. For example, comparing to the CD of hydrogel **1T**, the CD of the **1T**- $A_{10}$  mix gel (Fig. S5) exhibits the decreased ellipticity of positive band at 192, 228 nm and negative bands around

205, 247 and 287 nm regions. The CD spectrum of **3T**-A<sub>10</sub> mix gel (Fig. S5) shows that the addition of A<sub>10</sub> both changes the intensity of bands at 195, 205 nm and creates a new band at 303 nm that can be resulted from the conformational change of self-assembled structures of **3T** induced by A<sub>10</sub>. [14a-c] In addition, comparing to the solution of **1T** or **2T**, the CD spectra of the mix solution of A<sub>10</sub> with hydrogelator **1T** (or precursor **2T**) shows slight changes of the band shape, indicating the relatively weak interaction in the solution state (Fig. S5).

We also used molecular mechanical (MM) calculation to evaluate non-covalent interactions [15] and simulate the width of the nanofibers of **1**. As shown in Fig. 3a, the simulated widths of the nanofibers are 15 nm, 16 nm, 9 nm and 11 nm for nucleopeptides **1A**, **1G**, **1T** and **1C**, respectively, which correlate well with the trend in the experimental observation (Fig. 2). According to simulation, the thicker width of nanofibers in the hydrogels of **1A** and **1G** are likely resulted from the formation of Hoogsteen base pair [12, 16] by adenine or guanine nucleobases (Figs. S10 and S11). In addition, MM calculation supports the formation of  $\beta$ -sheet like structure.

To verify the biocompatibility of the hydrogelators, we added hydrogelator **1** or precursor **2** into the culture of HeLa cells and measured the proliferation of the cells. According to the MTT assay shown in Fig. 3, after being incubated with the 500  $\mu$ M of hydrogelator (**1A**, **1T**, or **1C**) or the precursor (**2A**, **2T**, or **2C**) for 72 hr, the cell viability remain at 100%. Although the cell viability decreases slightly when they are incubated with 500  $\mu$ M of **1G** or **2G** for 72 hr, the value of IC<sub>50</sub> is still > 500  $\mu$ M. These results prove that nucleopeptides **1**, **2**, and **3** are biocompatible. We also used a simple wound-healing assay [17] to examine the capability of the nanofibers and hydrogels of **3** to serve as a material for maintain cell-matrix interaction. As shown in Fig. 3d, the presence of the hydrogel of **3T** in cell culture has little inhibitory effect on the migration of cells, further supporting the biocompatibility of **3**.

Besides biocompatibility, biostability is also an essential requisite for a biomaterial. Thus, we examine the stability of hydrogelators by incubating them with proteinase K, a powerful protease that hydrolyzes a wide range of peptidic substrates and cleavage the peptide bond adjacent to the carboxyl group of aliphatic and aromatic amino acids with blocked alpha amino groups. [18] As shown in Fig. 4, more than 85 % of **2T**, **3T**, or **3A**, more than 70 % of **2A** or **3C**, and above 50% of **2C** remain after 24 hrs of the incubation with proteinase K; more than 40% of **2G** or **3G** remains after 4 hrs of the incubation with proteinase K. Although less than 10% of **1T** or Nap-FFY [19] remains after 4 hrs of the incubation with proteinase K (Fig. S13), the excellent or fair resistance to enzymatic digestion, exhibited by the nucleopeptides **2** and **3**, confirms the unique advantage of the nucleobases. Because of their high resistance to proteases, the hydrogel formed by hydrogelator **3T**, **3A**, or **3C** promises to serve as new biomaterials for applications that require long-term biostability. In addition, this result suggests that the incorporation of nucleobase may be an effective approach for improving the biostability of other small peptidic hydrogelators.

In conclusion, this work not only demonstrates the generation of a new type of hydrogelators based on the conjugates of nucleobases and short peptides that self-assemble in water to afford supramolecular hydrogels upon a pH- or enzymatic trigger, but also introduces a new, simple, and general approach for developing soft, biocompatible materials from nucleopeptides. Since it is easy to incorporate other bioactive peptides or molecular recognition motifs [20] with nucleobases, this work provides a facile way to explore the new applications of nucleopeptides as functional biomaterials.

## Supplementary Material

Refer to Web version on PubMed Central for supplementary material.

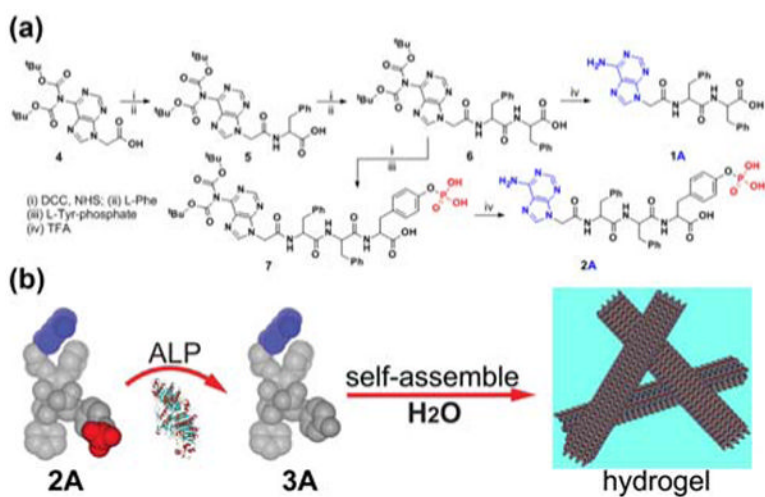
## Acknowledgments

This work was partially supported by NIH (R01CA142746), NSF (DMR 0820492), a HFSP grant (RGP0056/2008), and start-up grant from Brandeis University. The images were taken at Brandeis EM facilities.

## References

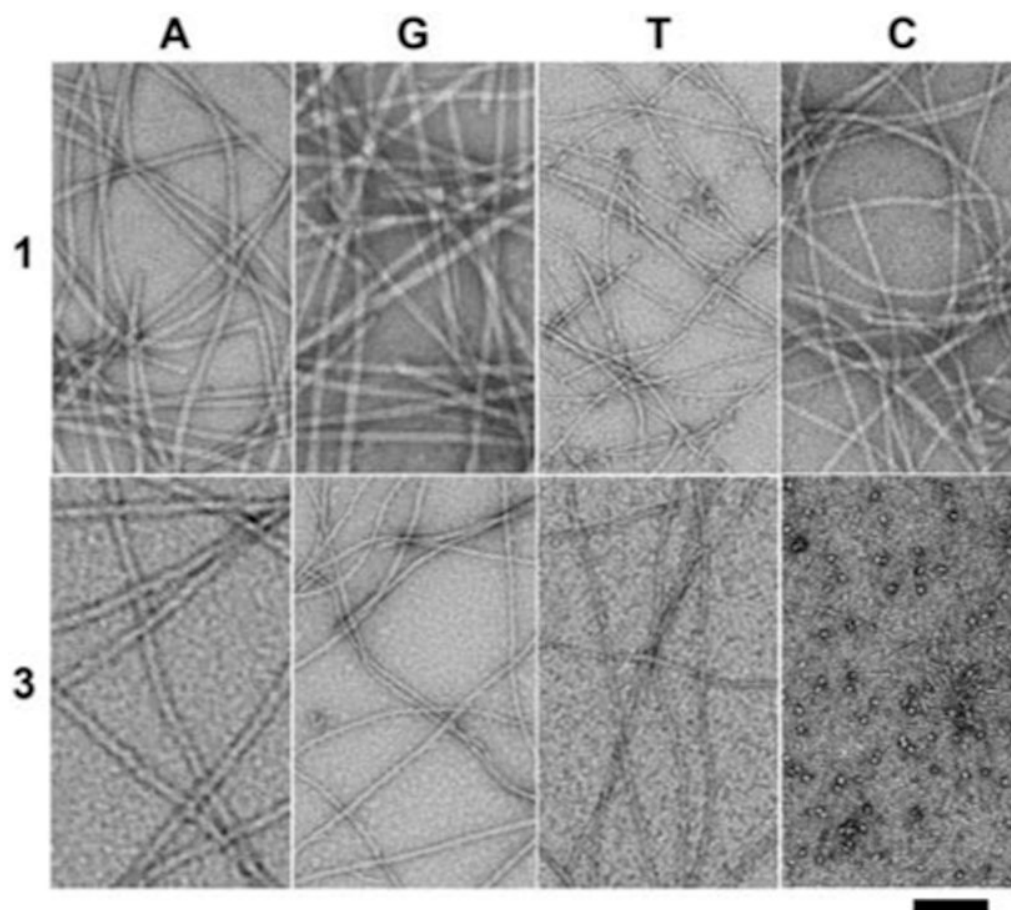
1. a) Roviello GN, Musumeci D, Bucci EM, Pedone C. *Mol Biosyst.* 2011; 7:1073. [PubMed: 21203614] b) Roviello GN, Benedetti E, Pedone C, Bucci EM. *Amino Acids.* 2010; 39:45. [PubMed: 20349320]
2. a) Azzam ME, Algranat Id. *Proc Natl Acad Sci USA.* 1973; 70:3866. [PubMed: 4590173] b) Hector RF, Zimmer BL, Pappagianis D. *Antimicro Agents Chemother.* 1990; 34:587.c) Itaya M, Yamaguchi I, Kobayashi K, Endo T, Tanaka T. *J Biochem.* 1990; 107:799. [PubMed: 2118136]
3. a) Nielsen PE, Egholm M, Berg RH, Buchardt O. *Science.* 1991; 254:1497. [PubMed: 1962210] b) Haaima G, Lohse A, Buchardt O, Nielsen PE. *Angew Chem Int Ed.* 1996; 35:1939.
4. a) Kool ET. *Acc Chem Res.* 2002; 35:936. [PubMed: 12437318] b) Pradeepkumar PI, Hobartner C, Baum DA, Silverman SK. *Angew Chem Int Ed.* 2008; 47:1753.c) Kool ET, Morales JC, Guckian KM. *Angew Chem Int Ed.* 2000; 39:990.
5. Nielsen PE. *Chem Biodivers.* 2010; 7:786. [PubMed: 20397216]
6. a) Iwaura R, Yoshida K, Masuda M, Ohnishi-Kameyama M, Yoshida M, Shimizu T. *Angew Chem, Int Ed.* 2003; 42:1009.b) Shimizu T, Iwaura R, Masuda M, Hanada T, Yase K. *J Am Chem Soc.* 2001; 123:5947. [PubMed: 11414828]
7. a) Estroff LA, Hamilton AD. *Chem Rev.* 2004; 104:1201. [PubMed: 15008620] b) Yang ZM, Gu HW, Fu DG, Gao P, Lam JK, Xu B. *Adv Mater.* 2004; 16:1440.c) Lee KY, Mooney DJ. *Chem Rev.* 2001; 101:1869. [PubMed: 11710233] d) Choi SW, Zhang Y, Xia YN. *Angew Chem Int Edit.* 2010; 49:7904.
8. a) Kiyonaka S, Sada K, Yoshimura I, Shinkai S, Kato N, Hamachi I. *Nat Mater.* 2004; 3:58. [PubMed: 14661016] b) Silva GA, Czeisler C, Niece KL, Beniash E, Harrington DA, Kessler JA, Stupp SI. *Science.* 2004; 303:1352. [PubMed: 14739465] c) Toledano S, Williams RJ, Jayawarna V, Ulijn RV. *J Am Chem Soc.* 2006; 128:1070. [PubMed: 16433511] d) Ulijn RV, Woolfson DN. *Chem Soc Rev.* 2010; 39:3349. [PubMed: 20672166] e) Valery C, Paternostre M, Robert B, Gulik-Krzywicki T, Narayanan T, Dedieu JC, Keller G, Torres ML, Cherif-Cheikh R, Calvo P, Artzner F. *Proc Natl Acad Sci USA.* 2003; 100:10258. [PubMed: 12930900] f) Wada A, Tamaru S, Ikeda M, Hamachi I. *J Am Chem Soc.* 2009; 131:5321. [PubMed: 19351208] g) Micklitsch CM, Knerr PJ, Branco MC, Nagarkar R, Pochan DJ, Schneider JP. *Angew Chem Int Ed.* 2011; 50:1577.
9. a) George M, Weiss RG. *Acc Chem Res.* 2006; 39:489. [PubMed: 16906745] b) Terech P, Weiss RG. *Chem Rev.* 1997; 97:3133. [PubMed: 11851487] c) Wang QG, Yang ZM, Zhang XQ, Xiao XD, Chang CK, Xu B. *Angew Chem Int Ed.* 2007; 46:4285.d) Yang Z, Liang G, Guo Z, Xu B. *Angew Chem Int Ed.* 2007; 46:8216.e) Li XM, Li JY, Gao YA, Kuang Y, Shi JF, Xu B. *J Am Chem Soc.* 2010; 132:17707. [PubMed: 21121607]
10. a) Gorbitz CH. *Chem Eur J.* 2001; 7:5153. [PubMed: 11775688] b) Gorbitz CH. *Chem Commun.* 2006:2332.c) Gorbitz CH. *Chem Eur J.* 2007; 13:1022. [PubMed: 17200919]
11. Porcheddu A, Giacomelli G, Piredda I, Carta M, Nieddu G. *Eur J Org Chem.* 2008:5786.
12. a) Araki, K.; Yoshikawa, I. *Low Molecular Mass Gelators: Design, Self-Assembly, Function.* Vol. 256. Springer-Verlag Berlin; Berlin: 2005. p. 133b) Davis JT. *Angew Chem, Int Ed.* 2004; 43:668.
13. Manning MC, Illangasekare M, Woody RW. *Biophys Chem.* 1988; 31:77. [PubMed: 3233294] b) N. W. Sreerama, R. W., (Ed.: N. Berova, Nakanashi, K., Woody, R. W.), Wiley-VCH, New York, **2000**, pp. p 601.
14. a) Arigon J, Prata CAH, Grinstaff MW, Barthelemy P. *Bioconjugate Chem.* 2005; 16:864.b) Dong GM, Zhang LR, Zhang LH. *Helv Chim Acta.* 2003; 86:3516.c) Godeau G, Bernard J, Staedel C, Barthelemy P. *Chem Commun.* 2009:5127.d) Iwaura R, Hoeben FJM, Masuda M, Schenning A,

- Meijer EW, Shimizu T. *J Am Chem Soc.* 2006; 128:13298. [PubMed: 17017812] e) Janssen PGA, Vandenberg J, van Dongen JJJ, Meijer EW, Schenning A. *J Am Chem Soc.* 2007; 129:6078. [PubMed: 17447768]
15. Mayo SL, Olafson BD, Goddard WA. *J Phys Chem.* 1990; 94:8897.
16. Sivakova S, Rowan SJ. *Chem Soc Rev.* 2005; 34:9. [PubMed: 15643486]
17. Rodriguez, LGWX.; Guan, JL. *Cell Migration: Developmental Methods and Protocols.* Guan, JL., editor. Vol. 294. Humana Press Inc.; Totowa, NJ: 2004. p. 23
18. a) Bromme D, Peters K, Fink S, Fittkau S. *Arch Biochem Biophys.* 1986; 244:439. [PubMed: 3511847] b) Liang GL, Yang ZM, Zhang RJ, Li LH, Fan YJ, Kuang Y, Gao Y, Wang T, Lu WW, Xu B. *Langmuir.* 2009; 25:8419. [PubMed: 20050040]
19. a) Yang Z, Liang G, Xu B. *Acc Chem Res.* 2008; 41:315. [PubMed: 18205323] b) Zhang Y, Kuang Y, Gao YA, Xu B. *Langmuir.* 2011; 27:529. [PubMed: 20608718]
20. Schneider HJ. *Angew Chem Intl Ed.* 2009; 48:3924.



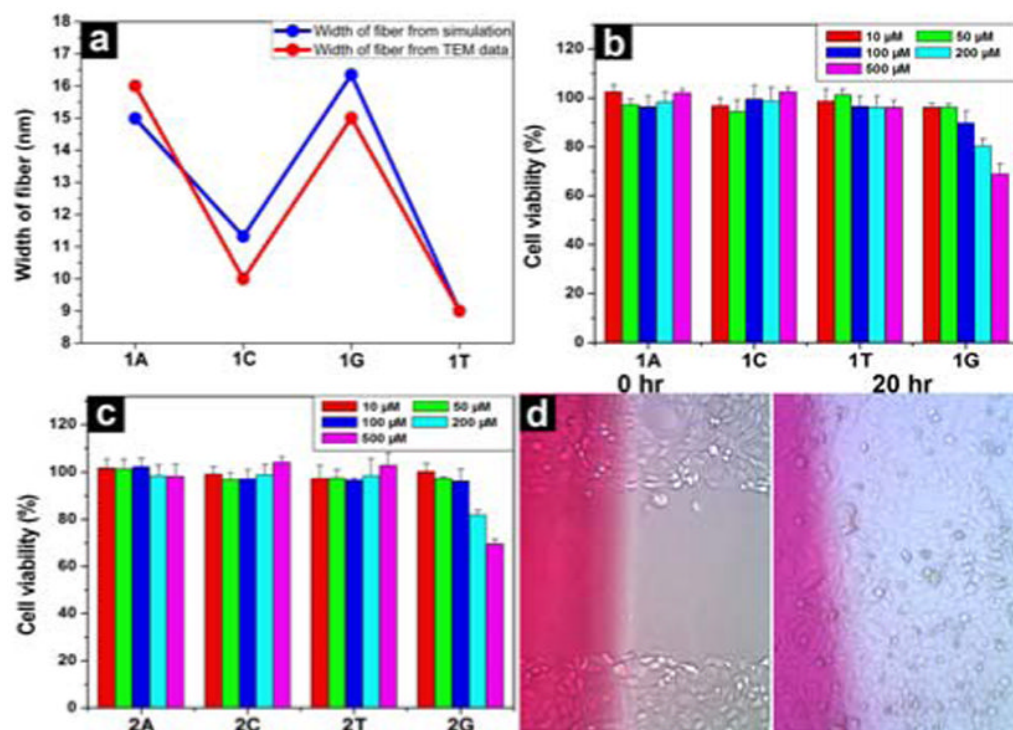
**Figure 1.**

(a) A typical synthetic route of a hydrogelator (**1A**) and a precursor (**2A**) based on adenine; (b) illustration of the dephosphorylation process catalyzed by alkaline phosphatase (ALP) that converts **2A** to **3A** and results in nanofibers and a hydrogel.



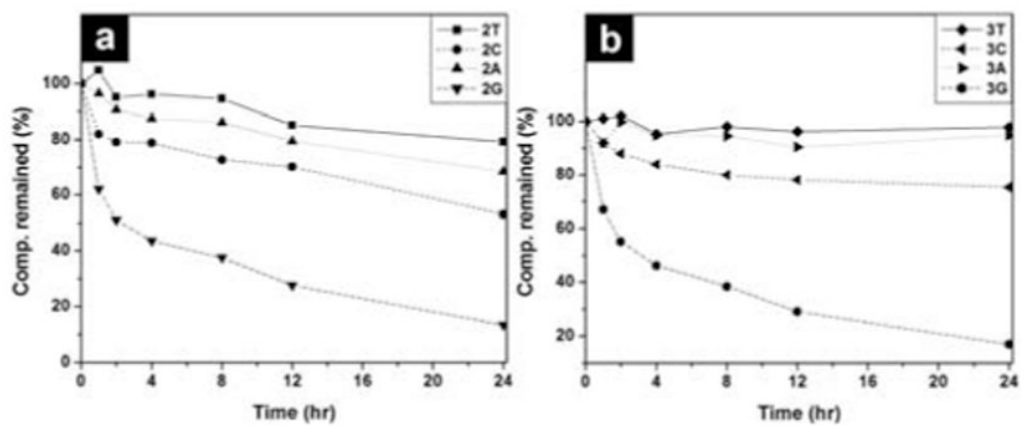
**Figure 2.** Transmission electron micrograph (TEM) of the hydrogels formed by **1A**, **1G**, **1T**, **1C**, **3A**, **3G**, **3T** and the solution of **3C** (scale bar = 100 nm).





**Figure 3.**

(a) A comparison of the width of fibers of hydrogels **1A**, **1C**, **1G** and **1T** based on transmission electron micrographs (in red) and molecular mechanical calculations (in blue). 72 hr cell viability test of (b) **1A**, **1C**, **1T** and **1G**; (c) **2A**, **2C**, **2T** and **2G**. (d) Optical images of HeLa cells on the surface 0 h and 20 h after the creation of scratch-wound in the presence of hydrogel **3T** (by adding 27.7 mM of **3T** in the media).





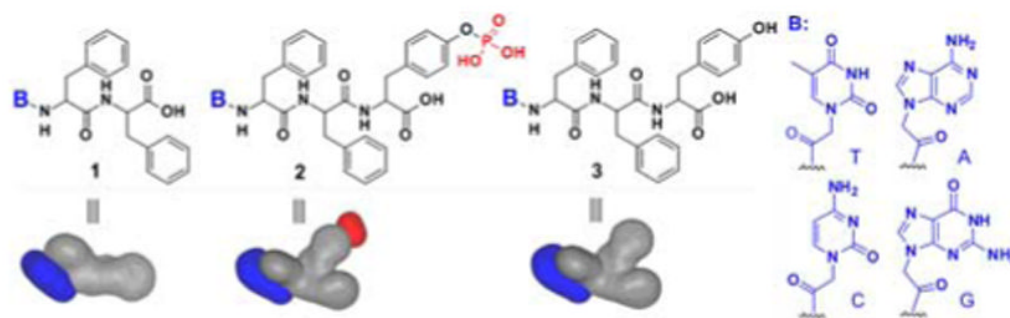






**Figure 4.** The time-dependent course of the digestions of hydrogelators of (a) 2T, 2C, 2G, 2A, and (b) 3T, 3A, 3G and compound 3C by proteinase K.

**Scheme 1.**

Molecular structures and shapes of the hydrogelators and corresponding precursors based on nucleopeptides.

**Table 1**  
The conditions and properties of the nucleopeptidic hydrogelators and corresponding supramolecular nanofibers and hydrogels.

Sample	1A	1G	1T	1C	3A	3G	3T	3C
wt %	2.0	2.0	2.0	2.0	2.0	2.0	2.0	2.0
pH	5.0	5.0	5.0	5.0	7.4	7.4	7.4	7.4
Optical images								
Width of nanofibers (nm)	16	15	9	10	20	14	95	5 <sup>a</sup>
Critical strain (%)	1.0	0.8	1.2	0.6	0.4	2.0	8.0	-
G' (pa)	8090	12613	6346	26	2082	682	2.9	-
IC <sub>50</sub> (μM)	>500	>500	>500	>500	>500	>500	>500	>500

<sup>a</sup>These thin nanofibers have low quantity and coexist with nanoparticles, thus fail to result in a hydrogel